Robust Extremes in Chaotic Deterministic Systems

Renato Vitolo, Mark P. Holland, Christopher A.T. Ferro
School of Engineering, Computing and Mathematics, University of Exeter (www.secam.ex.ac.uk/xcs/).

The concept

A chaotic deterministic system f_ρ has robust extremes under observable ϕ when the associated extreme value statistics depend smoothly on control parameter ρ.

Results

Robustness of extremes:

1. depends on system f_ρ and on observable ϕ;
2. allows improved estimates by pooling data and
3. improved prediction of (non-stationary) return levels.

Phenomenology

Robustness of extremes depends on the ***system*** f_ρ and on the ***observable*** ϕ.

Illustration for Lorenz63 model with $\sigma = 10$, $\beta = \frac{8}{3}$:

$$\dot{x} = \sigma(y - x), \quad \dot{y} = x(\rho - z) - y, \quad \dot{z} = xy - \beta z. \qquad (1)$$

For $\rho = 28$: (1) has robust strange attractor [1]. Let

$$\phi_1(x, y, z) = x, \qquad \phi_2(x, y, z) = 1 - |x - 5|^{0.25}. \qquad (2)$$

Generate time series of length 10^n units (recorded every 0.5) and extract maxima over blocks of 1000 time units. Fit generalised extreme value (GEV) distribution:

$$G(x; \mu, \sigma, \xi) = \exp\left[-\left(1 + \xi\frac{x - \mu}{\sigma}\right)_+^{-1/\xi}\right]. \qquad (3)$$

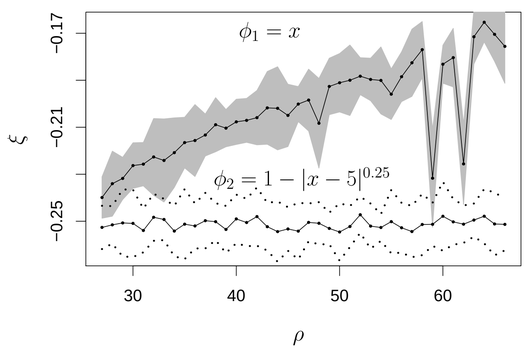

FIG. 1: Maximum likelihood estimates of ξ for observables ϕ_1 and ϕ_2 in (2), for $\rho_j = 27 + j$, $j = 0, 1, \ldots$

ϕ_1: for small ρ ($\approx$ 28), ξ varies smoothly with ρ. Nonlinear scaling of attractor $\rightsquigarrow$ shape of $\xi(\rho)$. Discontinuous for large ρ due to hyperbolicity loss (folds in return map).

ϕ_2: $\xi(\rho) = 0.25$ is constant even under hyperbolicity loss.

Rigorous proof available for 1D Lorenz maps.

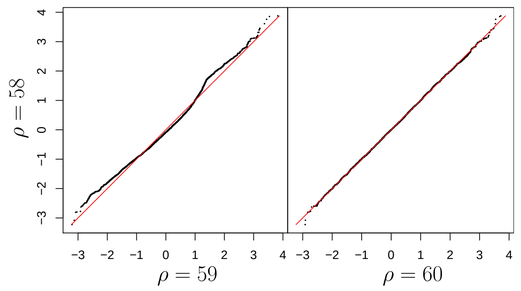

FIG. 2: Discontinuity in upper tail at $\rho = 59$ for ϕ_1 (quantile-quantile plot of 10^4 maxima from Fig 1, for each $\rho = 58, 59, 60$).

Pooling data

Robustness of extremes $\rightsquigarrow$ enhanced precision of GEV estimators.

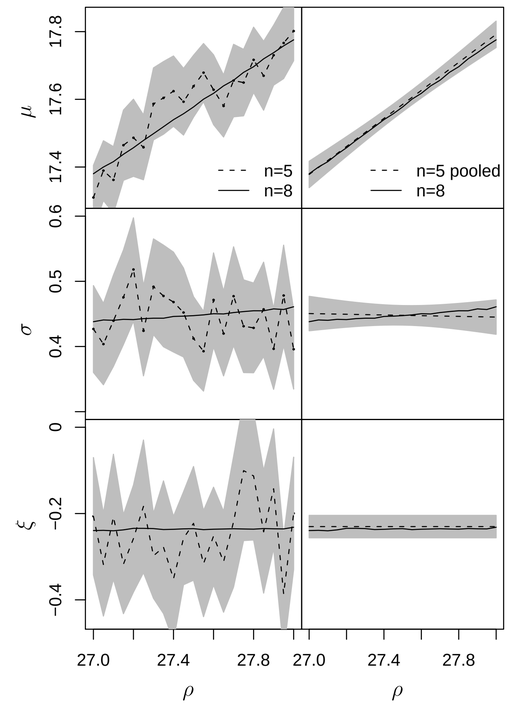

FIG. 3: Left: GEV parameter estimates for (1) with $n = 5$ (dashed, 95% conf. int. in gray) and $n = 8$ (solid). Right: "pooled" estimates with $n = 5$ (dashed, 95% conf. int. in gray).

Large n: GEV parameter estimates $\rightarrow$ smooth functions of ρ (solid lines in Fig 3, $n = 8$).
Small n: wild oscillations around "true values" (dashed lines, left column in Fig 3, $n = 5$).

Enhanced precision: "pooling" short series ($n = 5$)
Given robust extremes, information can be pooled from nearby ρ
$\rightsquigarrow$ reduction in uncertainty due to parameter estimation, cfr. grey bands in Fig 3. Assume functional forms

$$\mu(\rho) = \mu_0 + \mu_1\rho, \quad \sigma(\rho) = \sigma_0 + \sigma_1\rho, \quad \xi(\rho) = \xi_0.$$

ξ constant in ρ: approximation, only valid locally.
Estimate $(\mu_0, \mu_1, \sigma_0, \sigma_1, \xi_0)$ by maximum likelihood.

Prediction & non-stationarity

Robustness of extremes $\rightsquigarrow$ interpreting and predicting non-stationary extremes.

Robust extreme windspeeds are found in a simple two-layer quasi-geostrophic model [2]:
smooth dependence of windspeed return levels wrt baroclinic forcing parameter T_E in stationary case.

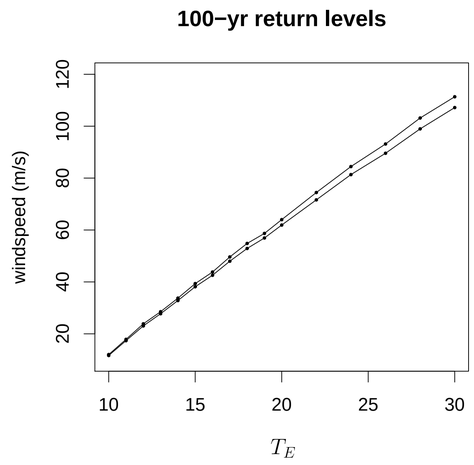

FIG. 4: 100-year windspeed return levels at centre of lower layer, for different values of T_E (non-pooled GEV fits, stationary case).

Introduce linear time trend in QG model:

$$T_E(t) = (T_E^0 - 1) + t\,\Delta T_E, \quad t \in [0, t_0], \quad \Delta T_E = 2/300 yrs.$$

Ansatzen: adiabatic + slow trend.

1. trend speed ΔT_E is sufficiently small wrt sampling time for upper tail of windspeed distribution;
2. non-stationary extremes remain close (locally in time) to those of stationary system for "frozen" $T_E(t)$.

$\Longrightarrow$ robustness of extremes wrt control parameter translates to smooth change of extremes wrt time.

We adopt the Generalized Additive Models for Location, Scale and Shape (GAMLSS) [3]:

1. response distribution is GEV with constant ξ and cubic smoothing spline for (μ, σ) with identity link;
2. split sequence of yearly maxima into training and test set (years 1-2250 and 2251-3000);
3. fit non-stationary GEV-GAMLSS to training set;
4. compute time-dependent quantiles and compare to training and test set.

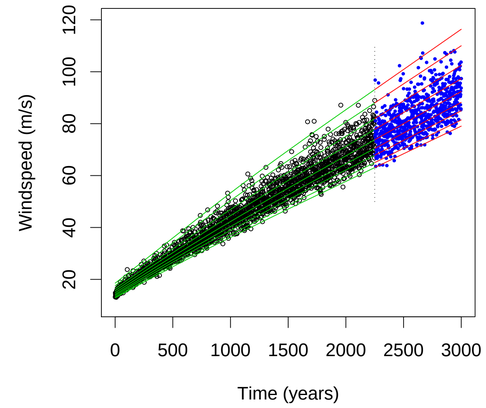

FIG. 5: Points: observed yearly windspeed maxima during training (black) and test (blue) periods. Curves: time-dependent estimated quantiles from GEV-GAMLSS.

quantiles	0.4	2	10	25	50	75	90	98	99.6
training	0.5	2.3	9.5	25.2	50.3	76.1	90.0	98.0	99.6
test	0.7	3.6	14.3	30.5	51.7	74.7	91.3	97.7	99.3

Fraction of points below the estimated quantile curves in Fig. 5 (corresp. to top row) during training (green, centre row) and test (red, bottom row) periods.

Illustrates potential for predicting return levels in a non-stationary system exhibiting robust extremes.

References

[1] Morales, C. A., Pacifico, M. J., and Pujals, E. R. *Proc. Amer. Math. Soc.* **127**(11), 3393–3401 (1999).

[2] Felici, M., Lucarini, V., Speranza, A., and Vitolo, R. *J. Atmos. Sci.* **64**(7), 2137–2158 Jul (2007).

[3] Rigby, R. A. and Stasinopoulos, D. M. *J. Roy. Statist. Soc. Ser. C* **54**(3), 507–554 (2005).